



This is a repository copy of *PDE-based deployment of multi-agent systems with enhanced leader communication and Wentzell boundary control*.

White Rose Research Online URL for this paper:

<https://eprints.whiterose.ac.uk/230328/>

Version: Accepted Version

Article:

Khansili, S. and Selivanov, A. orcid.org/0000-0001-5075-7229 (2025) PDE-based deployment of multi-agent systems with enhanced leader communication and Wentzell boundary control. *Systems & Control Letters*, 204. 106201. ISSN 0167-6911

<https://doi.org/10.1016/j.sysconle.2025.106201>

© 2025 The Authors. Except as otherwise noted, this author-accepted version of a journal article published in *Systems & Control Letters* is made available via the University of Sheffield Research Publications and Copyright Policy under the terms of the Creative Commons Attribution 4.0 International License (CC-BY 4.0), which permits unrestricted use, distribution and reproduction in any medium, provided the original work is properly cited. To view a copy of this licence, visit <http://creativecommons.org/licenses/by/4.0/>

Reuse

This article is distributed under the terms of the Creative Commons Attribution (CC BY) licence. This licence allows you to distribute, remix, tweak, and build upon the work, even commercially, as long as you credit the authors for the original work. More information and the full terms of the licence here:

<https://creativecommons.org/licenses/>

Takedown

If you consider content in White Rose Research Online to be in breach of UK law, please notify us by emailing eprints@whiterose.ac.uk including the URL of the record and the reason for the withdrawal request.



eprints@whiterose.ac.uk
<https://eprints.whiterose.ac.uk/>

PDE-Based Deployment of Multi-Agent Systems with Enhanced Leader Communication and Wentzell Boundary Control^{*}

Shubham Khansili^{*}, Anton Selivanov

School of Electrical and Electronic Engineering, The University of Sheffield, Sheffield, S1 3JD, The United Kingdom

ARTICLE INFO

Keywords:

Multi-agent systems
Partial differential equations
Linear matrix inequalities
Deployment problem

ABSTRACT

We present a deployment strategy for a multi-agent system (MAS) with a chain topology, where leader agents communicate and direct the system using controllers designed from a Partial Differential Equation (PDE) model. Both the leader and follower agents implement a consensus protocol, resulting in a system that can be modeled by a semilinear parabolic PDE. Based on this model, we design global controllers that utilize the information available to the leader agents, who can assess their deviation from the target position. By enhancing communication between the leaders, we achieve more accurate state estimation, which improves the performance of the global controllers. Additionally, we introduce a Wentzell-type boundary control, enabling the boundary agents to balance swarm cohesion with the deployment objective. We establish sufficient conditions for successful deployment, expressed as Linear Matrix Inequalities (LMIs). Numerical simulations show that the proposed global controllers outperform those used by non-communicating leaders.

1. Introduction

A multi-agent system (MAS) involves multiple agents working together to achieve specific goals, such as formation control, fault detection, learning, security, and task allocation [1]. The popular approach to modeling MAS involves using graph theory to represent agent interactions and ordinary differential equations (ODEs) to describe each agent's dynamics [2]. However, as the number of agents increases, this method can lead to unmanageable system representations and obscure system properties, resulting in a scalability problem (see [3; 4], and Remark 2.4 in [5]).

Models that employ partial differential equations (PDEs) can potentially resolve the scalability problem. It has long been observed that biological swarms (flocks of birds, schools of fish, and swarms of bees) resemble fluid-like entities rather than discrete ones, suggesting the use of continuum models for large-scale MAS [6; 7; 8; 9]. Since the complexity of the continuum model does not depend on the number of agents, they circumvent the scalability problem.

The control strategies for PDEs can be divided into boundary and in-domain actuation. The backstepping-based boundary controllers [10] have been adapted for MAS modeled by Burgers-type PDEs [11], parabolic PDEs [12; 13; 14; 15], and hyperbolic PDEs [16; 17]. Other types of boundary controllers were employed in [18] to ensure input-to-state stability of the wave equation, in [19] to address communication constraints in the 1D heat equation, and [21] to achieve the finite-time deployment of large-scale heterogeneous MAS with semi-Markov switching dynamics. The benefits of PDE-based modeling for MAS were emphasized in [20] with a single boundary leader.

Beyond boundary control, flatness-based motion planning was employed in [22] to achieve finite-time deployment in MAS governed by nonlinear PDEs, distributed in-domain control for dynamic average consensus was developed in [23], and a neural network-based adaptive consensus scheme was introduced in [24].


This paper adapts the in-domain control design for PDEs to solve the deployment problem for MAS. We focus on a MAS with a chain topology, where each agent knows its current and desired positions relative to its nearest neighbors. Using these local measurements, the agents implement a consensus protocol, leading to a system that can be modeled by a semilinear diffusion PDE. This PDE may exhibit instability, preventing the desired deployment. To address this instability, [25] and [5] adapted the spatial decomposition approach for in-domain PDE control, initially proposed by [26]. This approach uses leader agents who possess additional information that the swarm uses to obtain a piecewise constant state approximation for decision-making. That strategy assumed no communication between the leader agents.

This paper advances in-domain swarm deployment by incorporating inter-leader communication, which enables a more accurate approximation of the system state. To quantify the benefits of this enhanced estimation, we derive two bounds on the approximation error. The first bound recovers the estimate presented in [25], albeit with a different proof tailored to the piecewise linear approximation used by communicating leader agents. The second bound involves the second-order spatial derivative and gives an error bound that scales quadratically with the leader spacing. Consequently, the proposed approach is theoretically guaranteed to perform no worse than the method in [25], while offering potential improvements under mild smoothness assumptions.

In addition to allowing for inter-leader communications, we improve the boundary control design by introducing Wentzell boundary conditions, which involve both the

^{*} This work is funded by the School of Electrical and Electronic Engineering, University of Sheffield, through Research Training and Support Grant No. 319634.

^{*}Corresponding author

 skhansili1@sheffield.ac.uk (S. Khansili)

boundary value and its spatial derivative. In [25], dynamic Dirichlet-type boundary conditions were causing boundary agents to move aggressively toward the target. While this leads to fast convergence at the boundary, it often breaks coordination with interior agents, reducing swarm cohesion. Our Wentzell-based boundary control avoids this by maintaining smoother coupling between the boundary and the interior, which preserves overall cohesion and improves stability.

As a result of the above improvements, the presented method achieves faster convergence of agents to the desired target curve compared to [25], ensures that boundary leaders move cohesively with the interior of the swarm to maintain overall formation integrity, and reduces the number of leader agents required to achieve successful deployment.

Notations: We use $P < 0$ to denote that $P \in \mathbb{R}^{n \times n}$ is a negative-definite symmetric matrix, with symmetric elements sometimes represented by “*”. The Euclidean norm is denoted by $|\cdot|$, and the L^2 norm by $\|\cdot\|$. The Sobolev space H^1 is equipped with the norm $\|f\|_{H^1} = \sqrt{\|f\|^2 + \|f'\|^2}$. Partial derivatives are indicated using indices, e.g., $\partial z / \partial x = z_x$. The identity matrix of order n is denoted by I_n .

1.1. Preliminaries

Lemma 1 (Poincaré’s inequality, [27]). *If $g \in H^1(0, l)$ is such that $\int_0^l g(x)dx = 0$, then $\|g\| \leq \frac{l}{\pi} \|g'\|$.*

Lemma 2 (Wirtinger’s inequality, [28]). *If $g \in H_0^1(0, l)$, then $\|g\| \leq \frac{l}{\pi} \|g'\|$.*

Lemmas 1 and 2 were used in [29] and [26] to bound the error of the piecewise constant state approximation constructed using the averaged and point measurements. We will use the following Lemma 3 to bound the error of a piecewise linear approximation.

Lemma 3. *If $g \in H^2(0, l)$ with $g(0) = g(l) = 0$, then $\|g\| \leq \frac{l}{\pi} \|g'\| \leq \frac{l^2}{\pi^2} \|g''\|$.*

Proof. Since $g(0) = 0 = g(l)$, Wirtinger’s inequality implies $\|g\| \leq \frac{l}{\pi} \|g'\|$. Since $\int_0^l g'(x)dx = g(l) - g(0) = 0$, Poincaré’s inequality gives

$$\|g\| \leq \frac{l}{\pi} \|g'\| \leq \frac{l^2}{\pi^2} \|g''\|.$$

□

2. PDE-based control design for a MAS

Consider a multi-agent system (MAS) with $N + 1$ agents in \mathbb{R}^n governed by

$$\dot{z}_i(t) = f(t, z_i(t)) + u_i(t) + v_i(t), \quad i \in \mathcal{I} = \{0, 1, \dots, N\}, \quad (1)$$

where $z_i : [0, \infty) \rightarrow \mathbb{R}^n$ are the states of agents and $f : [0, \infty) \times \mathbb{R}^n \rightarrow \mathbb{R}^n$ describes the local dynamics. In Section 2.1, we design local controllers, $u_i : [0, \infty) \rightarrow \mathbb{R}^n$, that keep the agents close to one another and make the MAS

amenable to PDE-based modelling. Then, in Section 2.2, we employ the PDE model to design global controllers, $v_i : [0, \infty) \rightarrow \mathbb{R}^n$, that guarantee the desired global behavior, which is the agent deployment onto a given curve $\gamma \in C^2([0, 1], \mathbb{R}^n)$, i.e., $z_i(t) \rightarrow \gamma_i := \gamma(i/N)$ as $t \rightarrow \infty$. We solve the problem under the following assumptions:

- A1.** The function f is differentiable with respect to z and satisfies $|f_z(t, z)| \leq L$ for some $L > 0$. In particular, f is globally Lipschitz continuous in its second argument.
- A2.** Each agent $i \in \{1, \dots, N - 1\}$ measures its relative positions to the two nearest neighbors, $z_i(t) - z_{i-1}(t)$ and $z_i(t) - z_{i+1}(t)$, and knows its desired relative positions, $\gamma_i - \gamma_{i-1}$ and $\gamma_i - \gamma_{i+1}$. The boundary agents $i = 0$ and $i = N$ know the current and desired relative positions to the nearest neighbor $i = 1$ and $i = N - 1$. All the agents know their local dynamics on the target curve $f(t, \gamma_i)$.
- A3.** The leaders measure the differences between their states and their target positions on the curve, $z_i(t) - \gamma_i$.

Assumption **A1** guarantees that the MAS can be deployed using linear feedback with a large enough gain. Assumption **A2** implies that, if $z_{i-1}(t) = \gamma_{i-1}$ and $z_{i+1}(t) = \gamma_{i+1}$, then agent i can reach γ_i without knowing its absolute position. The agents also need to know $f(t, \gamma_i)$ to compensate the local dynamics on the target curve. Assumption **A3** is needed to achieve the desired absolute position of the MAS.

2.1. Local Controllers Design

All but the boundary agents, $i \in \mathcal{I} \setminus \{0, N\}$, locally implement the consensus protocol

$$u_i(t) = \frac{a}{h^2} [(z_{i+1}(t) - z_i(t)) - (\gamma_{i+1} - \gamma_i) + (z_{i-1}(t) - z_i(t)) - (\gamma_{i-1} - \gamma_i)] - f(t, \gamma_i) \quad (2)$$

with $h = 1/N$ and $a > 0$. Namely, agent i tries to keep its relative position to agents $i + 1$ and $i - 1$ as $\gamma_{i+1} - \gamma_i$ and $\gamma_{i-1} - \gamma_i$, respectively, while compensating for the local dynamics $f(t, \gamma_i)$ on the target curve. Substituting (2) into (1), we obtain

$$\dot{z}_i = \frac{a}{h^2} [(z_{i+1} - 2z_i + z_{i-1}) - (\gamma_{i+1} - 2\gamma_i + \gamma_{i-1})] + f(t, z_i) - f(t, \gamma_i) + v_i. \quad (3)$$

The idea of the PDE-based modelling of MAS is to introduce distributed state and control $z, v : [0, \infty) \times [0, 1] \rightarrow \mathbb{R}^n$ such that $z(t, ih) = z_i(t)$ and $v(t, ih) = v_i(t)$ for $i \in \mathcal{I}$ and $h = 1/N$. Then

$$z_{xx}(t, ih) \approx \frac{z_{i+1}(t) - 2z_i(t) + z_{i-1}(t)}{h^2}, \quad i \in \mathcal{I} \setminus \{0, N\}.$$

Similarly, the term with γ_i in (3) approximates γ_{xx} . Then, when $h \rightarrow 0$, i.e., $|\mathcal{I}| = N + 1 \rightarrow \infty$, (3) becomes ([30])

$$z_t(t, x) = a[z_{xx}(t, x) - \gamma_{xx}(x)] \\ + f(t, z(t, x)) - f(t, \gamma(x)) + v(t, x)$$

for $t \geq 0$ and $x \in (0, 1)$. The deployment error, $e(t, x) := z(t, x) - \gamma(x)$, satisfies

$$e_t(t, x) = ae_{xx}(t, x) + F(t, x, e) + v(t, x) \quad (4)$$

with $F(t, x, e) := f(t, \gamma(x) + e) - f(t, \gamma(x))$. Since f is Lipschitz continuous,

$$|F(t, x, e)| = |f(t, \gamma(x) + e) - f(t, \gamma(x))| \leq L|e|, \\ \forall t \geq 0, x \in [0, 1], e \in \mathbb{R}^n. \quad (5)$$

We assume that the boundary agents, $i \in \{0, N\}$, are leaders that implement the local controllers

$$u_0(t) = \frac{\sigma}{h}[(z_1(t) - z_0(t)) - (\gamma_1 - \gamma_0)] \\ - \kappa(z_0(t) - \gamma_0) - f(t, \gamma_0), \\ u_N(t) = -\frac{\sigma}{h}[(z_N(t) - z_{N-1}(t)) - (\gamma_N - \gamma_{N-1})] \\ - \kappa(z_N(t) - \gamma_N) - f(t, \gamma_N). \quad (6)$$

The term with $\sigma > 0$ couples the boundary leader to its nearest neighbor, aligning its motion with the local swarm behavior. Instead of moving independently toward the target, it stays coordinated with the group, improving cohesion. For example, if a boundary leader is on the target curve and $\sigma = 0$, it remains there even if its neighbor is far away, which weakens coordination. When $\sigma > 0$, it first moves towards the swarm, and then returns to the target along with the swarm, maintaining cohesion. The term with $\kappa > 0$ drives it towards the target position on the curve, while the term with f compensates local dynamics on the target curve.

Substituting (6) into (1) and taking $N \rightarrow \infty$, we obtain

$$e_t(t, 0) = -\kappa e(t, 0) + \sigma e_x(t, 0) + F(t, 0, e(t, 0)) + v(t, 0), \\ e_t(t, 1) = -\kappa e(t, 1) - \sigma e_x(t, 1) + F(t, 1, e(t, 1)) + v(t, 1). \quad (7)$$

Therefore, the designed local controllers (2) and (6) lead to a MAS with the deployment error whose dynamics are approximated by the PDE (4) with the boundary conditions (7). This approximation becomes more accurate when the number of agents, N , grows. Note that the space domain $x \in [0, 1]$ is selected for convenience. A different space domain would result in a different diffusion gain, which can be transformed into the considered case using the change of variables $\tilde{z}(x, t) = z(\alpha x, t)$.

2.2. Global Controller Design

Without the global controller ($v \equiv 0$), the error system (4), (7) may be unstable (e.g., for $F(t, e) = Le$ with large L) meaning that the MAS fails to deploy onto the target curve. The distributed state feedback $v(t, x) = -Ke(t, x)$ with large K would stabilize the system, but the deployment error $e(t, x)$ is not available since only the leaders know their positions relative to the target curve. Therefore, we construct a piecewise linear approximation of $e(t, x)$ using the leaders'

measurements. We place $M + 1 (\leq N + 1)$ leaders at $x_j \in \{ih\}_{i \in I} \subset [0, 1]$, $j = 0, \dots, M$, so that $x_0 = 0$ and $x_M = 1$. That is, $x_j = \sum_{k=1}^j \Delta_k$ for $j \geq 1$, where Δ_k is a multiple of h and is the spacing between two consecutive leaders. The maximum space between the leaders is $\Delta := \max_k \Delta_k$. The leaders provide the measurements

$$y_j(t) := e(t, x_j) = z(t, x_j) - \gamma(x_j), \quad j \in \{0, 1, \dots, M\}.$$

By communicating with each other, the leaders can construct the piecewise linear state approximation: For $x \in [x_j, x_{j+1}]$,

$$e(t, x) \approx y_j(t) + \frac{y_{j+1}(t) - y_j(t)}{\Delta_{j+1}}(x - x_j) \\ = y_j(t) \left(1 - \frac{x - x_j}{\Delta_{j+1}}\right) + y_{j+1}(t) \frac{x - x_j}{\Delta_{j+1}}.$$

Introducing

$$b_j(x) = \begin{cases} \frac{x - x_{j-1}}{\Delta_j}, & x \in [x_{j-1}, x_j], \\ \frac{x_{j+1} - x}{\Delta_{j+1}}, & x \in [x_j, x_{j+1}], \\ 0, & x \notin [x_{j-1}, x_{j+1}] \end{cases}$$

with $x_{-1} = 0$ and $x_{M+1} = 1$, we obtain

$$e(t, x) \approx \sum_{j=0}^M y_j(t) b_j(x). \quad (8)$$

This motivates the following global controller:

$$v(t, x) = -K \sum_{j=0}^M b_j(x) y_j(t) = -Ke(t, x) + Kv(t, x) \quad (9)$$

with a global controller gain $K > 0$ and approximation error $v(t, x) = e(t, x) - \sum_{j=0}^M y_j(t) b_j(x)$. Substituting (9) into (4) and (7), we obtained the closed-loop system

$$e_t(t, x) = ae_{xx}(t, x) + F(t, x, e) - Ke(t, x) + Kv(t, x), \quad (10)$$

accompanied by the boundary conditions

$$e_t(t, 0) = -(\kappa + K)e(t, 0) + \sigma e_x(t, 0) + F(t, 0, e(t, 0)), \\ e_t(t, 1) = -(\kappa + K)e(t, 1) - \sigma e_x(t, 1) + F(t, 1, e(t, 1)). \quad (11)$$

Now we derive two bounds on the approximation error $v(t, x)$. For $x \in [x_{j-1}, x_j]$,

$$v(t, x) = e(t, x) - y_{j-1}(t) b_{j-1}(x) - y_j(t) b_j(x)$$

since $b_i(x) = 0$ when $i \notin \{j-1, j\}$. Then, recalling that $y_j(t) = e(t, x_j)$, we obtain

$$v_x(t, x) = e_x(t, x) - e(t, x_{j-1}) b'_{j-1}(x) - e(t, x_j) b'_j(x) \\ = e_x(t, x) - \frac{e(t, x_j) - e(t, x_{j-1})}{\Delta_j} \\ = e_x(t, x) - \frac{1}{\Delta_j} \int_{x_{j-1}}^{x_j} e_s(t, s) ds.$$

Since $v(t, x_j) = 0$, Lemma 2 gives

$$\begin{aligned}
\|v(t, \cdot)\|_{[x_{j-1}, x_j]}^2 &\leq \frac{\Delta_j^2}{\pi^2} \|v_x(t, \cdot)\|_{[x_{j-1}, x_j]}^2 \\
&= \frac{\Delta_j^2}{\pi^2} \|e_x(t, \cdot) - \frac{1}{\Delta_j} \int_{x_{j-1}}^{x_j} e_s(t, s) ds\|_{[x_{j-1}, x_j]}^2 \\
&= \frac{\Delta_j^2}{\pi^2} \|e_x(t, \cdot)\|_{[x_{j-1}, x_j]}^2 \\
&\quad - \frac{2\Delta_j}{\pi^2} \int_{x_{j-1}}^{x_j} e_x(t, x) dx \int_{x_{j-1}}^{x_j} e_s(t, s) ds \\
&\quad + \frac{1}{\pi^2} \int_{x_{j-1}}^{x_j} [\int_{x_{j-1}}^{x_j} e_s(t, s) ds]^2 dx \\
&= \frac{\Delta_j^2}{\pi^2} \|e_x(t, \cdot)\|_{[x_{j-1}, x_j]}^2 - \frac{\Delta_j}{\pi^2} [\int_{x_{j-1}}^{x_j} e_x(t, x) dx]^2 \\
&\leq \frac{\Delta_j^2}{\pi^2} \|e_x(t, \cdot)\|_{[x_{j-1}, x_j]}^2 \leq \frac{\Delta_j^2}{\pi^2} \|e_x(t, \cdot)\|_{[x_{j-1}, x_j]}^2.
\end{aligned}$$

Since $\|v(t, \cdot)\|_{[0,1]}^2 = \sum_{j=1}^M \|v(t, \cdot)\|_{[x_{j-1}, x_j]}^2$, we have

$$\|v(t, \cdot)\|_{[0,1]}^2 \leq \frac{\Delta_j^2}{\pi^2} \|e_x(t, \cdot)\|_{[0,1]}^2. \quad (12)$$

Using Lemma 3 and the relation $b_j'' = 0$, we also have

$$\begin{aligned}
\|v(t, \cdot)\|_{[x_{j-1}, x_j]}^2 &\leq \frac{\Delta_j^4}{\pi^4} \|v_{xx}(t, \cdot)\|_{[x_{j-1}, x_j]}^2 \\
&= \frac{\Delta_j^4}{\pi^4} \|e_{xx}(t, \cdot)\|_{[x_{j-1}, x_j]}^2.
\end{aligned}$$

Therefore,

$$\|v(t, \cdot)\|_{[0,1]}^2 \leq \frac{\Delta_j^4}{\pi^4} \|e_{xx}(t, \cdot)\|_{[0,1]}^2. \quad (13)$$

Remark 1. If the leaders do not communicate, the piecewise linear approximation (8) can be replaced by a piecewise constant one where $b_j(x)$ are the characteristic functions of $[(x_j + x_{j-1})/2, (x_j + x_{j+1})/2]$. Then (12) still holds (with a simpler proof, see [26; 31]), but (13) does not. That is, communications between leaders allow for the bound (13), which improves the stability analysis as illustrated by the numerical simulations in Section 4.

2.3. Well-posedness of the closed-loop system

The well-posedness of (10), (11) with $\sigma = 0$ is established in a manner similar to [32, Section III.C]. Here, we consider the more difficult case when $\sigma \neq 0$. Introduce the Hilbert space

$$X = L^2(0, 1) \times \mathbb{R}^{2n}$$

with the scalar product: $\forall v_i = (f_i, \alpha_i) \in X$,

$$\langle v_1, v_2 \rangle_X = \langle f_1, f_2 \rangle_{L^2} + \frac{a}{\sigma} \alpha_1^T \alpha_2.$$

The boundary conditions (11) can be rewritten in the Wentzell form obtained by substituting the dynamics [33, Section 6]:

$$\begin{aligned}
ae_{xx}(t, 0) - \sigma e_x(t, 0) + \kappa e(t, 0) &= 0, \\
ae_{xx}(t, 1) + \sigma e_x(t, 1) + \kappa e(t, 1) &= 0.
\end{aligned}$$

Introduce an operator on X

$$\mathcal{G} \begin{bmatrix} f(\cdot) \\ f(0) \\ f(1) \end{bmatrix} = \begin{bmatrix} af''(\cdot) \\ \sigma f'(0) - \kappa f(0) \\ -\sigma f'(1) - \kappa f(1) \end{bmatrix}$$

with the domain

$$D(\mathcal{G}) = \left\{ \begin{bmatrix} f(\cdot) \\ f(0) \\ f(1) \end{bmatrix} \left| \begin{array}{l} f \in C^2[0, 1] \\ af''(0) - \sigma f'(0) + \kappa f(0) = 0 \\ af''(1) + \sigma f'(1) + \kappa f(1) = 0 \end{array} \right. \right\}.$$

By [34, Theorems 1.1], \mathcal{G} generates an analytic semigroup on X . The PDE (10), (11) can be written in the following abstract form

$$\frac{dE}{dt} = \mathcal{G}E + \mathcal{F}(t, E), \quad (14)$$

where $E(t) = \text{col}\{e(t, \cdot), e(t, 0), e(t, 1)\}$ and

$$\mathcal{F}(t, E) = \begin{bmatrix} F(t, \cdot, e(t, \cdot)) - K \sum_{j=0}^M b_j(x) e(t, x_j) \\ F(t, 0, e(t, 0)) - K e(t, 0) \\ F(t, 1, e(t, 1)) - K e(t, 1) \end{bmatrix}.$$

The scalar product in X was selected to ensure that \mathcal{G} is negative-definite and, therefore, $(-\mathcal{G})^{\frac{1}{2}}$ is well defined. Consider $X_{\frac{1}{2}} = D((-\mathcal{G})^{\frac{1}{2}})$ with the norm $\|E\|_{\frac{1}{2}} = \|(-\mathcal{G})^{\frac{1}{2}} E\|_X$. We show that $\mathcal{F} : X_{\frac{1}{2}} \rightarrow X$ is Lipschitz continuous. Since f is Lipschitz, the last two components of \mathcal{F} are Lipschitz and

$$\|F(t, \cdot, e_1(t, \cdot)) - F(t, \cdot, e_2(t, \cdot))\| \leq L \|e_1(t, \cdot) - e_2(t, \cdot)\|.$$

By the Sobolev embedding theorem (see, e.g., Lemma 3 of [35]), there exists C such that

$$\max_{x \in [0,1]} |e_1(t, x) - e_2(t, x)| \leq C \|e_1(t, \cdot) - e_2(t, \cdot)\|_{H^1}.$$

Since $K > 0$ and $\sum_{j=0}^M b_j(x) = 1$, this yields

$$\begin{aligned}
&\|K \sum_{j=0}^M b_j(\cdot) [e_1(t, x_j) - e_2(t, x_j)]\| \\
&\leq K \max_{x \in [0,1]} |e_1(t, x) - e_2(t, x)| \|\sum_{j=0}^M b_j(\cdot)\| \\
&\leq KC \|e_1(t, \cdot) - e_2(t, \cdot)\|_{H^1} \leq M \|E_1(t) - E_2(t)\|_{\frac{1}{2}}
\end{aligned}$$

for some $M > 0$. Therefore, \mathcal{F} is Lipschitz continuous. Then, [36, Theorem 6.3.1] guarantees that (14) has a unique solution

$$e \in C([0, T], L^2(0, 1)) \cap C^1((0, T), L^2(0, 1))$$

for $e(0, \cdot) \in H^1(0, 1)$. Since $\mathcal{F}(t, 0) = 0$, [36, Theorem 6.3.3] guarantees that $T = \infty$.

3. Stability Analysis

In this section, we derive stability conditions for the closed-loop error system, ensuring that agents converge to the target curve when their number is sufficiently large. In Section 3.1, we consider $\sigma > 0$, meaning the boundary leaders must account for swarm dynamics. If $\sigma = 0$, the conditions in Section 3.1 become infeasible. However, for a linear system, they can be modified to accommodate $\sigma = 0$, as shown in Section 3.2.

3.1. Stability of the nonlinear system

Theorem 1. Consider the closed-loop system (10), (11) with a diffusion coefficient $a > 0$, positive controller gains K , σ , and κ , maximum gap between leaders Δ , and nonlinearity F subject to (5). For a given decay rate $\delta \in (0, K)$, let there exist positive scalars p , μ , and λ_i , $i \in \{1, 2, 3\}$, such that

$$\mathcal{N} = \begin{bmatrix} \mathcal{N}_{11} & 0 & 1 & K \\ * & \mathcal{N}_{22} & -\mu & -\mu K \\ * & * & -\lambda_2 & 0 \\ * & * & * & \mathcal{N}_{44} \end{bmatrix} \leq 0, \quad (15)$$

$$\mathcal{M} = \begin{bmatrix} \mathcal{M}_{11} & \mathcal{M}_{12} & p \\ * & -2\sigma\mu & -\mu \\ * & * & -\lambda_3 \end{bmatrix} \leq 0, \quad (16)$$

where

$$\begin{aligned} \mathcal{N}_{11} &= -2(K - \delta) + \lambda_2 L^2, \\ \mathcal{N}_{22} &= -2\mu a + \lambda_1 \Delta^4 / \pi^4, \\ \mathcal{N}_{44} &= -\lambda_1 - 2(\mu(K - \delta) + a)\pi^2 / \Delta^2, \\ \mathcal{M}_{11} &= -2p(\kappa + K - \delta) + \lambda_3 L^2, \\ \mathcal{M}_{12} &= \sigma p + \mu\kappa - a. \end{aligned}$$

Then the closed-loop system (10), (11) is exponentially stable in the \mathcal{H}^1 norm with the decay rate δ , i.e.,

$$\exists C > 0: \|e(t, \cdot)\|_{\mathcal{H}^1} \leq C e^{-\delta t} \|e(0, \cdot)\|_{\mathcal{H}^1}. \quad (17)$$

Proof. Consider the Lyapunov functional

$$\begin{aligned} V &= V_1 + V_B, \\ V_1 &= \|e(t, \cdot)\|^2 + \mu \|e_x(t, \cdot)\|^2, \\ V_B &= p |\eta(t)|^2, \quad \eta(t) = \text{col}\{e(t, 0), e(t, 1)\}. \end{aligned} \quad (18)$$

Differentiating V_1 along the trajectories of (10), (11) and integrating by parts, we obtain

$$\begin{aligned} \dot{V}_1 &= 2\langle e(t, \cdot), e_t(t, \cdot) \rangle + 2\mu \langle e_x(t, \cdot), e_{xt}(t, \cdot) \rangle \\ &= 2\langle e(t, \cdot), e_t(t, \cdot) \rangle + 2\mu \left(e_x^T e_t \Big|_0^1 - \langle e_{xx}(t, \cdot), e_t(t, \cdot) \rangle \right) \\ &= 2 \int_0^1 (e - \mu e_{xx})^T (a e_{xx} + F - K e + K v) \\ &\quad - 2\sigma\mu |\eta_x|^2 - 2\mu(\kappa + K) e_x^T e \Big|_0^1 + 2\mu e_x^T F \Big|_0^1 \end{aligned} \quad (19)$$

with $\eta_x(t) = \text{col}\{e_x(t, 0), -e_x(t, 1)\}$. Integrating by parts, we obtain

$$2(a + \mu K) \int_0^1 e^T e_{xx} = 2(a + \mu K) \left(e^T e_x \Big|_0^1 - \|e_x(t, \cdot)\|^2 \right). \quad (20)$$

From (5), (12), and (13), we have

$$0 \leq \lambda_0 \left(\frac{\Delta^2}{\pi^2} \|e_x(t, \cdot)\|^2 - \|v(t, \cdot)\|^2 \right), \quad \lambda_0 > 0, \quad (21a)$$

$$0 \leq \lambda_1 \left(\frac{\Delta^4}{\pi^4} \|e_{xx}(t, \cdot)\|^2 - \|v(t, \cdot)\|^2 \right), \quad (21b)$$

$$0 \leq \lambda_2 \left(L^2 \|e(t, \cdot)\|^2 - \|F(t, \cdot, e(t, \cdot))\|^2 \right), \quad (21c)$$

$$0 \leq \lambda_3 \left(L^2 |\eta(t)|^2 - |\eta_F(t)|^2 \right), \quad (21d)$$

where $\eta_F(t) = \text{col}\{F(t, e(t, 0)), F(t, e(t, 1))\}$. Using (20) in (19), adding the right-hand sides of (21a)–(21c) to \dot{V}_1 , and taking $\lambda_0 = 2[\mu(K - \delta) + a]\frac{\pi^2}{\Delta^2}$ to zero the coefficient in front of $\|e_x(t, \cdot)\|^2$ (note that $\lambda_0 > 0$ since $K > \delta$), we obtain

$$\begin{aligned} \dot{V}_1 + 2\delta V_1 &\leq \int_0^1 \zeta^T(t, x) (\mathcal{N} \otimes I_n) \zeta(t, x) dx - 2\sigma\mu |\eta_x(t)|^2 \\ &\quad + 2(\mu\kappa - a) \eta^T(t) \eta_x(t) - 2\mu \eta_x^T(t) \eta_F(t), \end{aligned}$$

where $\zeta(t, x) = \text{col}\{e(t, x), e_{xx}(t, x), F(t, e), v(t, x)\}$. Differentiating V_B along the trajectories of (11), we find

$$\begin{aligned} \dot{V}_B + 2\delta V_B &\leq 2p \eta^T(t) \eta_t(t) + 2p\delta |\eta(t)|^2 + (21d) \\ &= (-2p(\kappa + K - \delta) + \lambda_3 L^2) |\eta(t)|^2 \\ &\quad + 2p\sigma \eta^T(t) \eta_x(t) + 2p \eta^T(t) \eta_F(t) - \lambda_3 |\eta_F(t)|^2. \end{aligned}$$

Setting $\zeta_B(t) = \text{col}\{\eta(t), \eta_x(t), \eta_F(t)\}$, we have

$$\begin{aligned} \dot{V} + 2\delta V &\leq \int_0^1 \zeta^T(t, x) (\mathcal{N} \otimes I_n) \zeta(t, x) dx \\ &\quad + \zeta_B^T(t) (\mathcal{M} \otimes I_{2n}) \zeta_B(t). \end{aligned}$$

Since $\mathcal{M} \leq 0$ and $\mathcal{N} \leq 0$, we have $\dot{V}(t) \leq -2\delta V(t)$, which implies $V(t) \leq e^{-2\delta t} V(0)$. By Lemma 3 of [35], $V_B(t) \leq c_B \|e(t, \cdot)\|_{H^1}^2$ for some c_B . Then,

$$c_1 \|e(t, \cdot)\|_{H^1}^2 \leq V(t) \leq c_2 \|e(t, \cdot)\|_{H^1}^2,$$

where $c_1 = \min\{1, \mu\}$ and $c_2 = \max\{1, \mu\} + c_B$. Therefore,

$$\|e(t, \cdot)\|_{H^1}^2 \leq \frac{V(t)}{c_1} \leq \frac{e^{-2\delta t}}{c_1} V(0) \leq \frac{c_2}{c_1} e^{-2\delta t} \|e(t, \cdot)\|_{H^1}^2,$$

which implies the exponential stability in the H^1 norm. \square

Remark 2. The conditions of Theorem 1 are feasible when L and Δ are sufficiently small, and K is sufficiently large. Moreover, if the conditions hold for some $\Delta = \Delta_F$, then they are feasible for all $\Delta \in (0, \Delta_F]$.

Proof. Since $\sigma > 0$, the relation

$$\mathcal{M}_{2:3} = \begin{bmatrix} -2\sigma\mu & -\mu \\ -\mu & -\lambda_3 \end{bmatrix} < 0$$

holds for a large enough $\lambda_3 > 0$. Then, by the Schur complement lemma, $\mathcal{M} < 0$ follows from

$$-2p(\kappa + K - \delta) + \lambda_3 L^2 + [\mathcal{M}_{12} \quad p] \mathcal{M}_{2:3}^{-1} [\mathcal{M}_{12} \quad p]^T < 0,$$

which holds for a large enough $K > 0$. Furthermore, the Schur complement lemma implies that $\mathcal{N} < 0$ if

$$\begin{bmatrix} \mathcal{N}_{11} & 0 \\ 0 & \mathcal{N}_{22} \end{bmatrix} - \begin{bmatrix} 1 & K \\ -\mu & -\mu K \end{bmatrix} \begin{bmatrix} \lambda_2^{-1} & 0 \\ 0 & \mathcal{N}_{44}^{-1} \end{bmatrix} \begin{bmatrix} 1 & -\mu \\ K & -\mu K \end{bmatrix} \leq 0.$$

Since $|\mathcal{N}_{44}| \rightarrow \infty$ when $\Delta \rightarrow 0$, the above holds for $L = 0$, large enough $\lambda_2 > 0$, and small enough $\Delta > 0$. By continuity, it remains true for a small enough $L > 0$.

To prove the second part, note that Δ appears only in the diagonal entries \mathcal{N}_{22} and \mathcal{N}_{44} , which decrease when Δ decreases. Therefore, if $\mathcal{N} \leq 0$, it remains so for smaller values of $\Delta > 0$. \square

3.2. Stability of the linear system

Theorem 1 cannot be used if $\sigma = 0$ because (16) becomes infeasible. However, the conditions can be adjusted to allow for $\sigma = 0$ if the system is linear, i.e., $f(t, z_i) = Lz_i$ in (1). In this case, the closed-loop error system (10), (11) with $F(e) = Le(t, x)$ simplifies to

$$\begin{aligned} e_t(t, x) &= ae_{xx}(t, x) - (K - L)e(t, x) + Kv(t, x), \\ e_t(t, 0) &= -(\kappa + K - L)e(t, 0) + \sigma e_x(t, 0), \\ e_t(t, 1) &= -(\kappa + K - L)e(t, 1) - \sigma e_x(t, 1). \end{aligned} \quad (22)$$

The following theorem provides simplified stability conditions that can be used with $\sigma = 0$, in which case they can be simplified further (see Corollary 1).

Theorem 2. Consider the closed-loop system (22) with a diffusion coefficient $a > 0$, reaction coefficient $L > 0$, and maximum gap between leaders Δ . For a given decay rate $\delta > 0$ and controller gains $K > L + \delta$, $\kappa > 0$, and $\sigma \geq 0$, let there exist positive scalars p , μ , and λ_1 such that

$$\tilde{\mathcal{N}} = \begin{bmatrix} \tilde{\mathcal{N}}_{11} & 0 & K \\ * & \tilde{\mathcal{N}}_{22} & -\mu K \\ * & * & \tilde{\mathcal{N}}_{33} \end{bmatrix} \leq 0, \quad (23)$$

$$\tilde{\mathcal{M}} = \begin{bmatrix} -2p(\kappa + K - L - \delta) & \sigma p + \mu\kappa - a \\ * & -2\sigma\mu \end{bmatrix} \leq 0, \quad (24)$$

where

$$\begin{aligned} \tilde{\mathcal{N}}_{11} &= -2(K - L - \delta), \\ \tilde{\mathcal{N}}_{22} &= -2\mu a + \lambda_1 \Delta^4 / \pi^4, \\ \tilde{\mathcal{N}}_{33} &= -\lambda_1 - 2[\mu(K - L - \delta) + a]\pi^2 / \Delta^2. \end{aligned}$$

Then the closed-loop system (22) is exponentially stable in the \mathcal{H}^1 norm with the decay rate δ in the sense of (17).

Proof. Consider the Lyapunov functional V defined in (18). Calculations similar to (19) give

$$\begin{aligned} \dot{V}_1 &= 2 \int_0^1 (e - \mu e_{xx})^T (ae_{xx} - (K - L)e + Kv) \\ &\quad - 2\sigma\mu|\eta_x|^2 - 2\mu(\kappa + K - L)e_x^T e \Big|_0^1 \end{aligned}$$

with $\eta_x(t) = \text{col}\{e_x(t, 0), -e_x(t, 1)\}$. Integrating by parts, adding the right-hand sides of (21a) and (21b), and taking $\lambda_0 = 2[\mu(K - L - \delta) + a]\frac{\pi^2}{\Delta^2}$ to zero the coefficient in front of $\|e_x(t, \cdot)\|^2$, we obtain

$$\dot{V}_1 + 2\delta V_1 \leq \int_0^1 \bar{\xi}^T (\tilde{\mathcal{N}} \otimes I_n) \bar{\xi} + 2(a - \mu\kappa)e_x^T e \Big|_0^1 - 2\sigma\mu|\eta_x|^2,$$

where $\bar{\xi}(t, x) = \text{col}\{e(t, x), e_{xx}(t, x), v(t, x)\}$. Differentiating V_B along the trajectories of (22), we find

$$\begin{aligned} \dot{V}_B + 2\delta V_B &= 2p\eta^T(t)\eta_t(t) + 2p\delta|\eta(t)|^2 \\ &= [-2p(\kappa + K - L - \delta)]|\eta(t)|^2 + 2p\sigma\eta^T(t)\eta_x(t). \end{aligned}$$

Setting $\bar{\xi}_B(t) = \text{col}\{\eta(t), \eta_x(t)\}$, we have

$$\begin{aligned} \dot{V} + 2\delta V &\leq \int_0^1 \bar{\xi}^T(t, x)(\tilde{\mathcal{N}} \otimes I_n)\bar{\xi}(t, x) dx \\ &\quad + \bar{\xi}_B^T(t)(\mathcal{M} \otimes I_{2n})\bar{\xi}_B(t). \end{aligned}$$

Therefore, (23) and (24) guarantee $\dot{V} \leq -2\delta V$. The rest of the proof is similar to that of Theorem 1. \square

Corollary 1. Consider the closed-loop system (22) with a diffusion coefficient $a > 0$, reaction coefficient $L > 0$, and maximum gap between leaders Δ . Given controller gains $K > L + \delta$, $\kappa > 0$, and $\sigma = 0$, let there exist a positive λ_1 such that (23) holds with $\mu = a/\kappa$. Then the closed-loop system (22) is exponentially stable in the \mathcal{H}^1 norm with the decay rate δ in the sense of (17).

Proof. If $\sigma = 0$, then (24) holds for $\mu = a/\kappa$. If (23) holds for this μ , then the conditions of Theorem 2 are satisfied, implying the exponential stability of (22). \square

Remark 3. The conditions of Theorem 2 and Corollary 1 are feasible when Δ is sufficiently small and K is sufficiently large. The proof is similar to Remark 2.

4. Numerical Simulations

Consider the MAS (1) with 41 agents ($N = 40$), each having a three-dimensional state ($n = 3$). Let the control objective be to deploy the agents from $(0, 0, 0)$ onto the target curve $\gamma(s) = (1.5 \sin s, 1.5 \cos s, 6)$, $s \in [0, 1]$. We consider two cases: (i) linear local dynamics, $f(t, z_i) = Lz_i$, and (ii) non-linear local dynamics, $f(t, z_i) = L \sin(z_i)$. In both scenarios, local controllers u_i are designed according to (2) for interior agents and (6) for boundary agents. These controllers rely on agents measuring their relative positions to immediate neighbors, which is susceptible to noise. To mitigate the impact of noise, we select a small interaction gain a . The resulting error dynamics can be described by the PDE (10), (11). Using this PDE model, we design global controllers of the form $v_i = v(t, i/N)$ with v defined in (9).

In Section 4.1, we demonstrate that the control strategy proposed in this paper for interacting leaders requires fewer leaders compared to the control strategy developed for non-communicating leaders. Note that stability conditions for non-interacting leaders are given by Theorems 1 and 2 with $\lambda_1 = 0$ since (13) does not hold in this case (see Remark 1). Then, in Section 4.2, we highlight the benefits of choosing $\sigma > 0$, which leads to Wentzell boundary conditions and forces boundary leaders to account for the swarm dynamics.

Table 1

Allowable leader spacing Δ from Theorem 2, with and without leader communication, for (25) and various a .

Local controller gain a	0.001	0.004	0.01	0.14
Communicating leaders	0.08	0.17	0.27	1
Non-communicating leaders	0.04	0.08	0.14	0.53

4.1. Enhanced connectivity requires fewer leaders

Consider the linear error system (22) with

$$K = 1.4, \quad \kappa = 1, \quad \sigma = 6, \quad L = 0.3, \quad \delta = 1. \quad (25)$$

Table 1 presents the maximum values of Δ for different choices of a such that the LMIs of Theorem 2 are feasible. In all cases, inter-leader communication allows for larger Δ , implying that fewer leaders are required to successfully deploy the MAS. Specifically, for $a = 4 \times 10^{-3}$, we obtain $\Delta \leq 0.17$, meaning that seven leaders are needed: $1 + 1/0.17 \approx 6.8$. Without inter-leader communication, the feasible value decreases to $\Delta \leq 0.08$, requiring twice as many leaders: $1 + 1/0.08 \approx 13.5$. Table 2 further illustrates that, across various parameter configurations, enabling inter-leader communication consistently reduces the number of leaders needed for stabilization. Similarly, Table 3 provides admissible values of Δ for the nonlinear system, confirming that inter-leader communication allows for fewer leaders.

Figures 1 and 2 show the maximum feasible values of Δ from Theorems 1 and 2, respectively, for interacting and non-interacting leader cases, versus local control gain a . As a increases, the feasible Δ also increases, indicating that fewer leaders are needed for stability. For instance, when $a = 0.14$, then $\Delta = 1$, meaning the system can be stabilized using only two boundary leaders (see Figure 2 and Table 1). Since the spatial domain is normalized to $[0, 1]$, Δ must lie in the interval $0 < \Delta \leq 1$. Notably, $\Delta = 1$ remains feasible for all $a \geq 0.14$.

Table 4 shows how the allowable leader spacing Δ varies with the global gain K . For small K , the effect of the approximation error $Kv(t, x)$ in (10) is moderate, so using a more accurate piecewise linear approximation significantly improves performance, allowing larger Δ and fewer leaders. As K increases, even small estimation errors are amplified, reducing the advantage of improved approximation. Both strategies then yield similar Δ , and the difference between communicating and non-communicating leaders narrows. For very large K , the LMIs become infeasible.

4.2. Wentzell boundary control improves stability

Using the parameter values in (25) (with $a = 0.004$), Figure 3 shows the corresponding boundary error evolution $\log \|e(t, 0)\|$ and $\log \|e(t, 1)\|$ for $\sigma = 0$ and $\sigma > 0$, and Figure 4 shows the evolution of $\log \|e(t, \cdot)\|$ for four scenarios: $\sigma = 6$ with (orange) and without (dashed-orange) leader communication, and $\sigma = 0$ with (red) and without (dashed-red) communication. Figure 3 shows that with $\sigma = 0$ the boundary leaders reach the target faster than in the Wentzell case, yet Figure 4 makes clear that this faster

Table 2

Required number of leaders with and without communication for various system parameters with $a = 0.01$, based on LMIs in Theorem 2.

Global controller gain, K	5	2.1	2	1.5	1
Boundary controller gain κ	4	1	2	3	2
Boundary controller gain σ	1	2	1	1	4
Decay rate, δ	2	1	0.8	1	0.4
Lipschitz constant, L	2	1	1	0.4	0.5
Communicating leaders	7	6	6	5	4
Non-communicating leaders	10	13	9	9	7

Table 3

Allowable leader spacing Δ from Theorem 1, with and without leader communication, for $K = 1$, $\kappa = 2$, $\sigma = 6$, $L = 0.1$, $\delta = 0.8$, and various a .

Local controller gain a	0.001	0.01	0.1	0.25
Communicating leaders	0.13	0.24	0.78	1
Non-communicating leaders	0.10	0.19	0.62	0.99

Table 4

Allowable leader spacing Δ from Theorem 2, for different values of K , with and without leader communication ($a = 0.01$; other parameters as in (25)).

Global gain K	1.31	1.45	5	10000
Communicating leaders	0.27	0.27	0.24	Infeas.
Non-communicating leaders	0.04	0.16	0.24	Infeas.

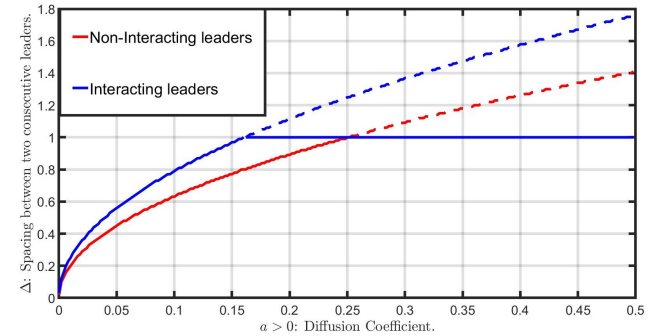


Figure 1: Plot of Δ versus a from Theorem 1 for $K = 1$, $\kappa = 2$, $\sigma = 6$, $L = 0.1$, and $\delta = 0.8$.

boundary motion does not improve overall performance: the global error decays slower for both communicating and non-communicating leaders (solid and dashed red) than for their Wentzell counterparts (solid and dashed orange). Thus, regardless of leader communication, Wentzell boundary control ($\sigma > 0$) yields lower error and stronger cohesion. Communication among leaders further accelerates convergence, irrespective of the boundary control used, as the solid curves consistently outperform their dashed counterparts. The combination of communication among leaders and Wentzell control therefore delivers the best overall convergence.

Figure 5 shows that $\log \|e(\cdot, t)\|$ converges faster with 7 communicating leaders than with 7 non-communicating

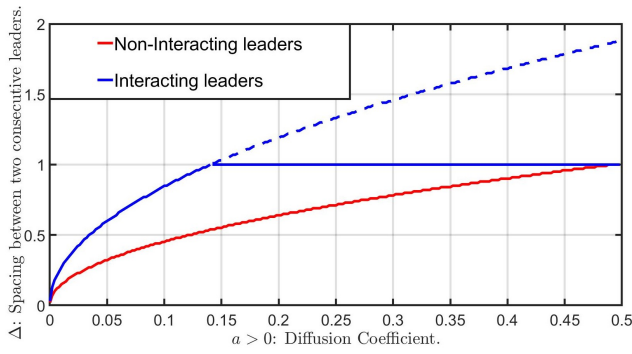


Figure 2: Plot of Δ versus a from Theorem 2 for (25).

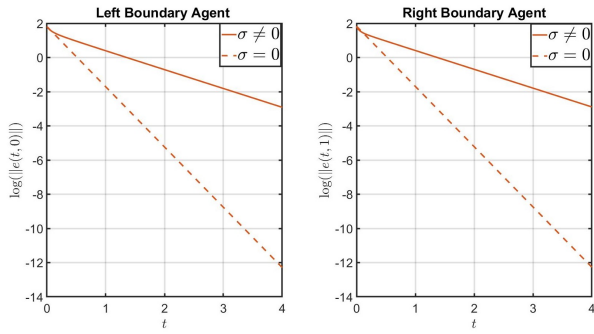


Figure 3: Evolution of $\log(\|e(t, x)\|)$ against t from (22), at $x = 0$ and $x = 1$ for $\sigma \neq 0$ and $\sigma = 0$.

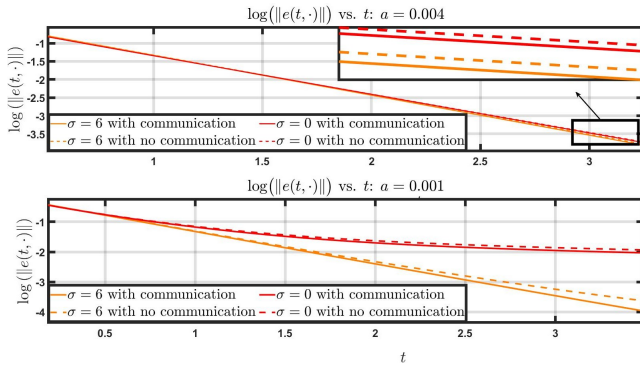


Figure 4: Plot of $\log(\|e(t, \cdot)\|)$ against t from (22), considering $\sigma = 6$ or $\sigma = 0$, with and without communication among seven leaders, for $a = 0.004$ (Top) and $a = 0.001$ (Bottom).

leaders. In the non-communicating case, at least 14 leaders are required to theoretically guarantee the deployment using Theorem 2 with $\lambda_1 = 0$ (see Table 1 with $a = 0.004$). As evident from the figure, the 7-leader communication strategy performs better than the 12 non-communicating leaders, highlighting the efficiency of leader interaction.

Figure 6 shows the target curve (orange) and the trajectories of 41 agents (black), including seven leaders with $i = 0, 7, 13, 20, 27, 33, 41$ (yellow) for the parameters in (25) and $a = 4 \times 10^{-3}$. Figure 7 depicts the effect of the control gain, σ , with and without leader communication. As expected, interacting leaders always outperform isolated leaders. Furthermore, larger value of σ improves

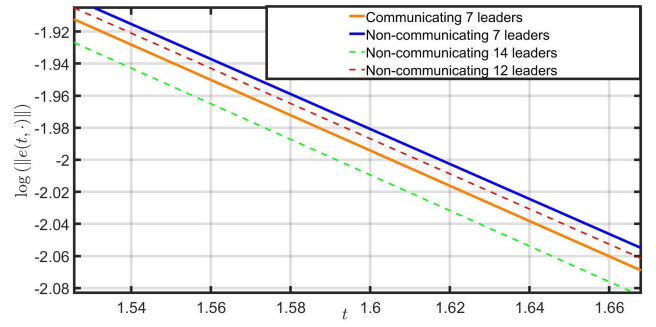


Figure 5: Plot of $\log(\|e(t, \cdot)\|)$ vs t given by (22) under Wentzell boundary control with and without leader communication for different numbers of leaders.

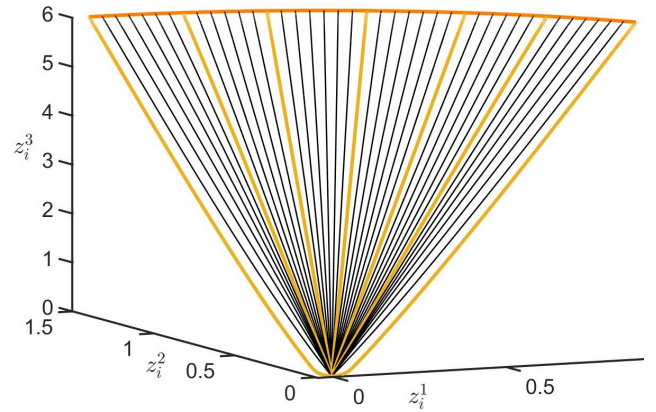


Figure 6: Phase-portrait for 41 agents with 7 leaders (yellow) and target curve (orange).

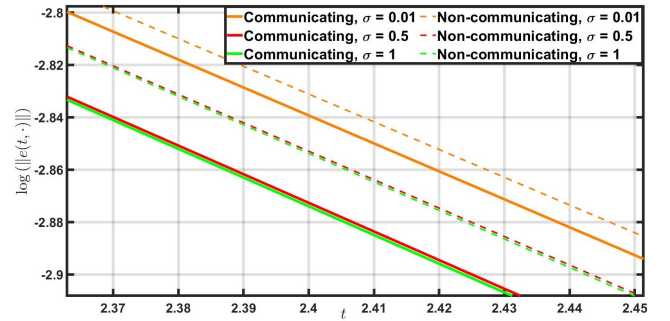


Figure 7: The deployment error given by (22) under the Wentzell boundary control for different values of σ .

convergence. Figures 8 and 9 show 3D surface plots of the deployment error $e(t, x)$ for 7 leaders with and without communication, respectively (with parameter values in (25)). The deployment error decreases faster with communication, highlighting the critical role of leader interaction in improving performance.

5. Conclusion

We demonstrated how PDE-based modeling of large-scale MAS can enhance agent deployment by taking advantage of inter-leader communications. These communications

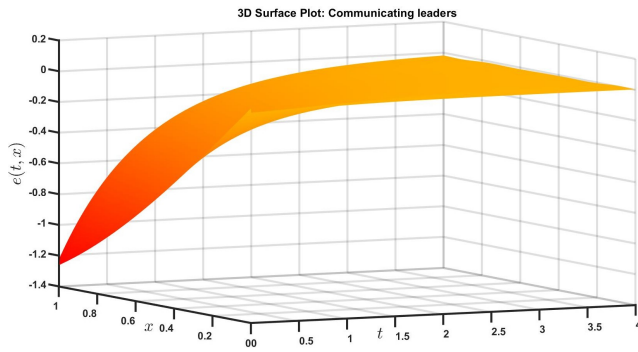


Figure 8: 3D surface plot of PDE (22), using (25), $a = 0.004$, and 7 communicating leaders.

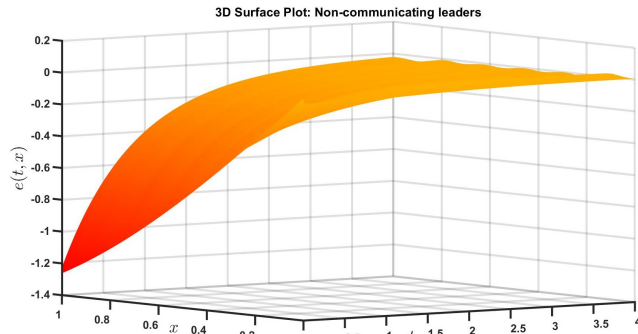


Figure 9: 3D surface plot of PDE (22), using (25), $a = 0.004$, and 7 non-communicating leaders.

enable a piecewise linear approximation of the state, with its error bounded using Wirtinger's and Poincaré's inequalities. This bound informs the Lyapunov-based analysis, leading to linear matrix inequalities that ensure convergence of the deployment error. Numerical simulations showed that, in some cases, inter-leader communications reduce the required number of leader agents by 50%. Additionally, we highlighted the advantages of Wentzell-type boundary control, which compels boundary agents to account for swarm dynamics. The results were derived for both linear and semilinear PDEs, with simulations confirming the benefits of inter-leader communications and Wentzell boundary control.

The authors declare that they have no known competing financial interests or personal relationships that could have appeared to influence the work reported in this paper.

No data was used for the research described in the article.

References

- [1] A. Dorri, S. S. Kanhere, and R. Jurdak, "Multi-agent systems: A survey," *IEEE Access*, vol. 6, pp. 28 573–28 593, 2018.
- [2] R. Olfati-Saber, J. A. Fax, and R. M. Murray, "Consensus and cooperation in networked multi-agent systems," *Proceedings of the IEEE*, vol. 95, no. 1, pp. 215–233, 2007.
- [3] C. W. Reynolds, "Flocks, herds and schools: A distributed behavioral model," in *Proceedings of the 14th annual conference on Computer graphics and interactive techniques*, 1987, pp. 25–34.
- [4] J. Lunze, *Feedback control of large-scale systems*. Prentice Hall New York, 1992.
- [5] M. Terushkin and E. Fridman, "Network-based deployment of non-linear multi agents over open curves: A PDE approach," *Automatica*, vol. 129, p. 109697, 2021.
- [6] J. Toner and Y. Tu, "Long-range order in a two-dimensional dynamical XY model: how birds fly together," *Physical review letters*, vol. 75, no. 23, p. 4326, 1995.
- [7] G. Flierl, D. Grünbaum, S. Levin, and D. Olson, "From individuals to aggregations: the interplay between behavior and physics," *Journal of Theoretical Biology*, vol. 196, no. 4, pp. 397–454, 1999.
- [8] T. Vicsek and A. Zafeiris, "Collective motion," *Physics reports*, vol. 517, no. 3–4, pp. 71–140, 2012.
- [9] H. Rastgoftar and S. Jayasuriya, "Evolution of multi-agent systems as continua," *Journal of Dynamic Systems, Measurement, and Control*, vol. 136, no. 4, p. 041014, 2014.
- [10] M. Krstic and A. Smyshlyaev, *Boundary control of PDEs: A course on backstepping designs*. SIAM, 2008.
- [11] G. Freudenthaler, F. Göttsch, and T. Meurer, "Backstepping-based extended Luenberger observer design for a Burgers-type PDE for multi-agent deployment," *IFAC-PapersOnLine*, vol. 50, no. 1, pp. 6780–6785, 2017.
- [12] P. Frihauf and M. Krstic, "Leader-enabled deployment onto planar curves: A PDE-based approach," *IEEE Transactions on Automatic Control*, vol. 56, no. 8, pp. 1791–1806, 2010.
- [13] J. Qi, R. Vazquez, and M. Krstic, "Multi-agent deployment in 3-D via PDE control," *IEEE Transactions on Automatic Control*, vol. 60, no. 4, pp. 891–906, 2014.
- [14] G. Freudenthaler and T. Meurer, "PDE-based multi-agent formation control using flatness and backstepping: Analysis, design and robot experiments," *Automatica*, vol. 115, p. 108897, 2020.
- [15] S. Wang, M. Diagne, and J. Qi, "Delay-adaptive compensation for 3-D formation control of leader-actuated multi-agent systems," *Automatica*, vol. 164, p. 111645, 2024.
- [16] P. Barooah, P. G. Mehta, and J. P. Hespanha, "Mistuning-based control design to improve closed-loop stability margin of vehicular platoons," *IEEE Transactions on Automatic Control*, vol. 54, no. 9, pp. 2100–2113, 2009.
- [17] J. Qi, J. Zhang, and Y. Ding, "Wave equation-based time-varying formation control of multiagent systems," *IEEE Transactions on Control Systems Technology*, vol. 26, no. 5, pp. 1578–1591, 2017.
- [18] L. Aguilar, Y. Orlov, and A. Pisano, "Leader-follower synchronization and ISS analysis for a network of boundary-controlled wave PDEs," *IEEE Control Systems Letters*, vol. 5, no. 2, pp. 683–688, 2021.
- [19] R. Katz, E. Fridman, and I. Basre, "Network-based deployment of multi-agents without communication of leaders with multiple followers: A PDE approach," in *2022 IEEE 61st Conference on Decision and Control (CDC)*, 2022, pp. 6089–6096.
- [20] A. Selivanov and E. Fridman, "PDE-based deployment of multiagents measuring relative position to one neighbor," *IEEE Control Systems Letters*, vol. 6, pp. 2563–2568, 2022.
- [21] J. Man, Y. Sheng, C. Chen, and Z. Zeng, "PDE-based finite-time deployment of heterogeneous multi-agent systems subject to multiple asynchronous semi-markov chains," *IEEE Transactions on Circuits and Systems I: Regular Papers*, vol. 71, no. 2, pp. 885–897, 2023.
- [22] T. Meurer and M. Krstic, "Finite-time multi-agent deployment: A nonlinear PDE motion planning approach," *Automatica*, vol. 47, no. 11, pp. 2534–2542, 2011.
- [23] M. Hasanzadeh and S.-X. Tang, "Dynamic average consensus as distributed PDE-based control for multi-agent systems," in *2024 European Control Conference (ECC)*. IEEE, 2024, pp. 828–833.
- [24] X. Shang, L. Tang, Y.-J. Liu, and S. Zhang, "Adaptive control for parabolic PDE based multi-agent systems," *International Journal of Control*, vol. 98, no. 4, pp. 815–823, 2025.
- [25] J. Wei, E. Fridman, and K. H. Johansson, "A PDE approach to deployment of mobile agents under leader relative position measurements," *Automatica*, vol. 106, pp. 47–53, 2019.
- [26] E. Fridman and A. Blighovsky, "Robust sampled-data control of a class of semilinear parabolic systems," *Automatica*, vol. 48, no. 5, pp. 826–836, 2012.

- [27] L. E. Payne and H. F. Weinberger, "An optimal poincaré inequality for convex domains," *Archive for Rational Mechanics and Analysis*, vol. 5, no. 1, pp. 286–292, 1960.
- [28] G. H. Hardy, J. E. Littlewood, and G. Pólya, *Inequalities*. Cambridge university press, 1952.
- [29] E. Fridman and N. B. Am, "Sampled-data distributed H_∞ control of a class of parabolic systems," in *2012 IEEE 51st IEEE Conference on Decision and Control (CDC)*. IEEE, 2012, pp. 7529–7534.
- [30] G. Ferrari-Trecate, A. Buffa, and M. Gati, "Analysis of coordination in multi-agent systems through partial difference equations," *IEEE Transactions on Automatic Control*, vol. 51, no. 6, pp. 1058–1063, 2006.
- [31] A. Selivanov and E. Fridman, "Distributed event-triggered control of diffusion semilinear PDEs," *Automatica*, vol. 68, pp. 344–351, 2016.
- [32] S. Khansili and A. Selivanov, "PDE-based deployment with communicating leaders for a large-scale multi-agent system," in *2023 European Control Conference (ECC)*. IEEE, 2023, pp. 1–6.
- [33] A. Favini, G. R. Goldstein, J. A. Goldstein, and S. Romanelli, "The heat equation with generalized Wentzell boundary condition," *Journal of evolution equations*, vol. 2, no. 1, pp. 1–19, 2002.
- [34] F. Colombo, A. Favini, and E. Obrecht, "Generation of analytic semigroups with generalized Wentzell boundary condition," in *Semigroup Forum*, vol. 90. Springer, 2015, pp. 615–631.
- [35] W. Kang and E. Fridman, "Distributed delayed stabilization of Korteweg–de Vries–Burgers equation under sampled in space measurements," in *Proceedings of the 23rd International Symposium on Mathematical Theory of Networks and Systems*, 2018.
- [36] A. Pazy, *Semigroups of linear operators and applications to partial differential equations*. Springer Science & Business Media, 2012, vol. 44.